Modeling and Simulation of a Side-Port Regenerative Glass Furnace

Hamzeh, M. H. and Sadrameli, Sayed Mojtaba*[+]

Department of Chemical Engineering, Tarbiat Modarres University, P.O. Box 14115-143, Tehran, I.R. IRAN

ABSTRACT: *A mathematical model for the performance prediction of an industrial glass furnace with six ports on each side was developed. This model comprises of two main sub-models for the combustion chamber and glass-melting tank. The first sub-model consists of the models for the combustion and the heat transfer model including, radiation, convection and conduction. The fuel combustion in atmospheric pressure is assumed perfectly and without soot. Heat balance equations in the gas; glass and walls determine the rate of heat transfer to the glass surface. The second sub-model consists of the model for the batch melting. The temperature distribution in the glass tank is computed by using results of the combustion simulation and effective conduction coefficient of molten glass. The results of the combustion model can be used for the pollution prediction and optimization of the furnace parameters to decrease the gas pollutants in the furnace.*

KEY WORDS: *Glass furnace, Modeling, Simulation, Combustion, Regenerator, Optimization*

INTRODUCTION

There is currently considerable industrial interest in support of the development of a mathematical model, which reliably simulates the performance of a glass-melting furnace. The reasons for this interest are two folds. First, glass furnaces are large and so they are extremely costly to develop by highly empirical methods. Second, interest is glass purity. Most often use of gas-fire giving rise to the hope that straightforward and existing modeling can be utilized to provide an adequate description of the turbulent flow, combustion and heat transfer processes.

Most of the previous works in this area have been reported in the literature. McConnell and Goodson [1] presented a simplified model in which global energy equations for the combustion chamber, glass melt and feed were solved for an assumed flow and heat release. Hottel's [2] employed zone method be to calculate the combustion chamber radiation. Mase and Oda [3] used a similar method to solved the flow field in the glass melts assuming two-dimensional model. A three dimensional simulation of a glass furnace combustion chamber has been developed [4] in which the flow field and heat release were determined from the numerical solution of the model. Sun and Song [5] have also simulated a glass furnace in which they simplified the combustion model by assuming the uniform heat flux

* *To whom correspondence should be addressed.*

[+] *E-mail: sadramel@modares.ac.ir*

1021-9986/04/2/81 8/$/2.80

on the melting glass surface.

Wang, Brewster and Mc Quay [6] developed a coupled model for the combustion space and melting glass and validated the results with an industrial glass furnace. This work presents the results of the simulation for a side-port regenerative industrial glass furnace. The mathematical model including three sub-models for the radiation, glass melting port and the regenerative exchangers of the furnace has been developed to optimize the furnace operation. The combined glass furnace and regenerator models and the effects of air pre-heating on the furnace performance have been developed for the first time. The results of the combustion model can be used for the pollution prediction and optimization of the furnace parameters to decrease the gas pollutants in the furnace.

Furnace Characteristics

The furnace is the side-port regenerative type with six ports on each side (each port containing two fuel jets). Natural gas fuel is admitted from six ports situated in the sidewalls of the furnace. The flame forms a loop within the combustion chamber and exits through the partner port. The nominal capacity of the furnace is 380 tons per day of molten glass. The furnace dimensions are 12m length, 8m width, and 2m height with 1.5m molten glass height. The ports are situated in two meter apart.

MATHEMATICAL MODEL

The present model includes four sub-models for the radiation heat transfer, combustion, regenerative exchangers of the furnace and the batch melting. All four models were linked together to perform a unique mathematical model for the simulation of the furnace.

Radiation Model

Due to the very high temperature (1600-1800 °K) of the furnace, radiation is the main heat transfer mechanism in the furnace. For the simulation of the furnace, the zone method of Hottel and Sarofim [2] has been utilized. The furnace walls and volume have been divided to 24 volume and 68 surface zones of two meters size as shown in Fig. 1. For the radiation model the wall and melting surface emmisivity coefficients have been considered as 0.7 and 0.8 respectively.

Table 1: Input data

Total fuel flow = 16.06 gmole/sec
Fuel temperature = 298 °K
Percent of excess air = 10
The capacity of furnace = 380 tons/day of molten glass
The flame-direction reversal time (t_b) = 20 minutes
The flame-cycle time (t_c) = 39 sec

Table 2:. The output data

Adiabatic temperature of flame = 2549.52 °K
The temperature of inlet gas to the regenerator = 1845.85 °K
The temperature of outlet gas from the regenerator = 745.37 °K
The mole percent of combustion products in the flue gas: H_2O = 18.413 CO_2 = 8.631 CO = 0.01909 H_2 = 0.010418 O_2 = 1.722 OH = 0.06116 N_2 = 71.01 NO_x = 0.13288

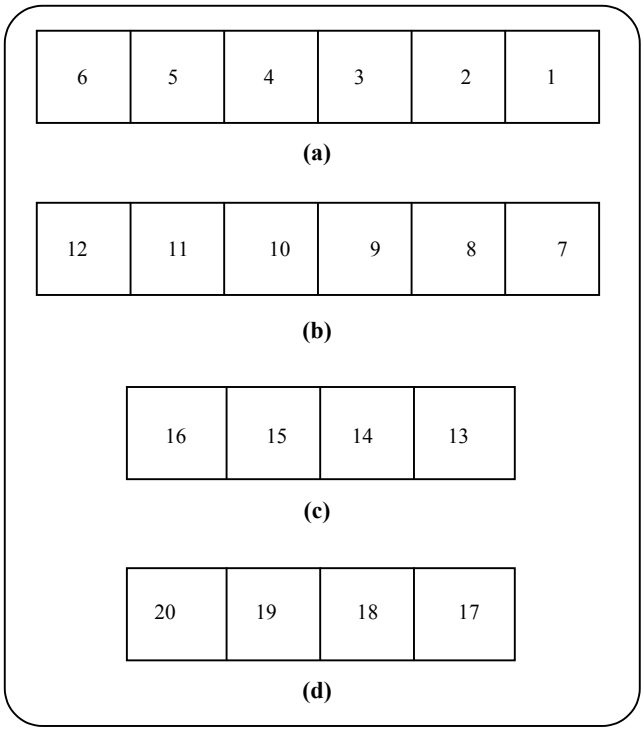

Fig. 1: Numbering of the parts of the furnace side walls a:burners, b: outlet hot gas windows, c: side walls on the width

Zone Method [7]

If the temperature distribution is available for the entire furnace, a radiative energy balance can be written for each zone (finite volumes and surfaces). The radiative balance includes the exchange of heat between a given zone and every other zone in the system. This is done with the help of the *directed flux areas* which can be defined as a measure of the way the given zone or another zone in both the ways directly and indirectly due to reflections from the surrounding zones. If the gaseous medium is gray, the net radiative exchange between a pair of zones is formulated as:

$$\dot{Q}_{i\Leftrightarrow j} = \overrightarrow{S_iS_j}\, E_{s,i} - \overleftarrow{S_iS_j}\, E_j \qquad (1)$$

$$\dot{Q}_{i\Leftrightarrow j} = \overrightarrow{G_iS_j}\, E_{g,i} - \overleftarrow{G_iS_j}\, E_j$$

$$\dot{Q}_{i\Leftrightarrow j} = \overrightarrow{G_iG_j}\, E_{g,i} - \overleftarrow{G_iG_j}\, E_j$$

Where $\overrightarrow{S_iS_j}$, $\overrightarrow{G_iS_j}$ and $\overrightarrow{G_iG_j}$ are the directed flux areas between two surface zones, a gas and a surface zone, or two gas zones, respectively. These are dependent solely on I) geometry and radiative properties (e.g. position of a zone relative to another, absorption coefficient of the intervening gas between two gas zones, and emmisivity of surface zones), II) they are dependent of temperature.

Considering the interactions between a surface zone *i* and all the other zones *j* of the furnace, the net radiative heat flow on surface zone *i* can be expressed as:

$$\dot{Q}_{s,i(net)} = \sum_j \overrightarrow{S_jS_i}\, E_{s,j} + \sum_j \overrightarrow{G_jS_i}\, E_{g,j} - A_i\varepsilon_i E_{s,i} \qquad (2)$$

In the radiative balance of gas zone *i* we considering all the interactions with the other zones of the furnace, including itself, is given by:

$$\dot{Q}_{g,i(net)} = \sum_j \overrightarrow{G_jG_i}\, E_{g,j} + \sum_j \overrightarrow{S_jG_i}\, E_{s,j} - 4K_iV_iE_{g,i} \qquad (3)$$

Combustion Model

The combustion model is based on the ideal of a single step and fast reaction between the gaseous fuel (natural gas) and oxidant, assume to combine in stoichiometric proportion. The fuel combustion in atmospheric pressure is assumed perfectly and without any soot. Three gray plus one clear gas model the combustion products. Determination of mole fraction of combustion products is gained from the mole balance on the elements and equilibrium equations of products.

$C_mH_n + a\,(1 + X)(O_2 + 3.76\ N_2) \rightarrow b_1CO_2 + b_2CO + b_3H_2O + B_4H_2 + b_5OH + B_6O_2 + b_7B_2 + b_8NO$

Mole balance on the elements:

$$m=b_1 + b_2 \qquad (4)$$

$$n=2b_3 + 2b_4 + b_5 \qquad (5)$$

$$2a(1+X)=2b_1+ b_2 + b_3 + b_5 + 2b_6 + b_8 \qquad (6)$$

$$2\times3.76\times a(1+X)=2b_7 + b_8 \qquad (7)$$

Equilibrium equations:

$$H_2O \Leftrightarrow H_2 + 1/2\ O_2 \qquad K_{p,1} = \frac{y_{H_2}\cdot y_{O_2}^{1/2}}{y_{H_2O}}\, pt^{1/2} \qquad (8)$$

$$H_2O \Leftrightarrow 1/2\ H_2 + OH \qquad K_{p,2} = \frac{y_{H_2}^{1/2}\, y_{OH}}{y_{H_2O}}\, pt^{1/2} \qquad (9)$$

$$CO_2 \Leftrightarrow CO + 1/2\ O_2 \qquad K_{p,3} = \frac{y_{CO}\cdot y_{O_2}^{1/2}}{y_{CO_2}}\, pt^{1/2} \qquad (10)$$

$$1/2\ N_2 + 1/2\ O_2 \Leftrightarrow NO \qquad K_{p,4} = \frac{y_{NO}}{y_{N_2}^{1/2}\cdot y_{O_2}^{1/2}} \qquad (11)$$

Theoretical Model of Regenerators [8]

The regenerator mathematical model developed in this work is based on the following assumptions;

1-Constant fluid and solid physical properties throughout the periods

2-Constant heat transfer coefficient during the periods

3-Constant and uniform velocity profile in the fluid phase

4-Constant fluid mass flow rates

5-No heat dispersion in the fluid

6-No radiation heat transfer in the system

7-No heat loss through and within the system

8-Solid thermal conductivity is zero parallel to the flow and infinite in the normal direction.

Because of the great length of regenerators and spherical shaped packing which having only one contact point with each other, one may assume that the solid thermal conductivity in the direction of flow is zero. The radial thermal conductivity may be assumed as same definition of lumped heat transfer coefficient as proposed by Hausen [9].

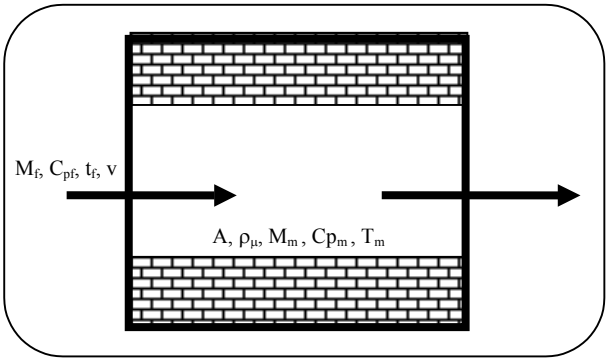

Fig. 2: Fixed-bed regenerator flow channel

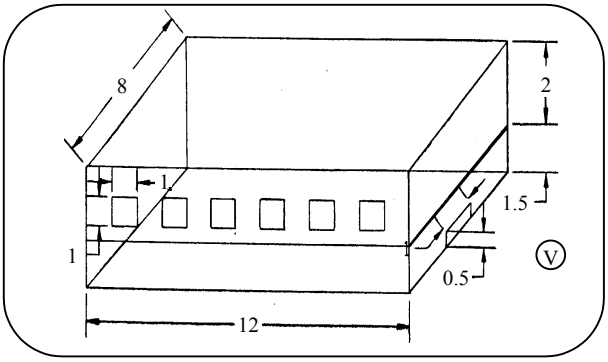

Fig. 3: Dimensions and zones of the furnace

The model is based on the partial differential equations representing the spatial and temporal variations of the temperature of the fluid, T_f, and of the material forming the regenerator matrix, T_m. Consider the flow of fluid of specific heat C_{pf} at a rate $\dot{M}_f$ through one channel of a regenerator containing a mass of material M_m of specific heat C_{pm} (Fig. 2). At this stage it is assumed that the material thermal conductivity is infinitely large in the direction perpendicular to the axis of flow and zero in the direction parallel to the axis. In other words, at any axial position, x, the temperature of the material, T_m, is uniform and equal to the surface temperature, T_s.

The surface area of the channel, *A*, and the lumped heat transfer coefficient between the fluid and the surface, $\bar{\alpha}$, is assumed to be uniform and invariant with time. The velocity of the fluid, υ, given by

$$\upsilon = \frac{\dot{M}_f}{S\rho_t} \tag{12}$$

Where S is the cross-sectional area of the flow passage and is also assumed to be constant. If the fluid is being heated by the solid ($T_s \rangle T_f$), the rate of heat transfer over length *dx* at position *x* and time *t* is given by

$$d\dot{Q} = \bar{\alpha} A(T_s - T_f)\frac{dx}{L} \tag{13}$$

$$d\dot{Q} = (\dot{M}_f C_{pf} L\frac{\partial T_f}{\partial x} + M_f C_{pf}\frac{\partial T_f}{\partial t}) \tag{14}$$

Where

$$M_f = \rho_f SL = \dot{M}_f\frac{L}{\upsilon}$$

Which can be expressed as

$$d\dot{Q} = \dot{M}_f C_{pf}(\frac{\partial T_f}{\partial x} + \frac{1}{\upsilon}\frac{\partial T_f}{\partial t})dx \tag{15}$$

Hence from equation (5),

$$\bar{\alpha} A(T_s - T_f) = \dot{M}_f C_{pf} L(\frac{\partial T_f}{\partial x} + \frac{1}{\upsilon}\frac{\partial T_f}{\partial t}) \tag{16}$$

The first term in the parentheses represents the increase in sensibility heat of fluid as it flows through the channel, and the second term represents the effect of the heat capacity of fluid resident in the channel.

The heat is transferred from the solid, causing a reduction in temperature with time given by;

$$-d\dot{Q} = \frac{M_m C_{pm}}{L}\frac{\partial T_m}{\partial t} \tag{17}$$

Equations (16) and (18) are the basic relationships used in the design of regenerators. Unfortunately, gaining an analytical solution is very difficult in a regenerator therefore approximate techniques will supplement or replace the analytical solutions. The non linear equations resulted from the energy balances have been solved by the Newton-Raphson numerical method.

Batch Melting Model [5]

The batch melting mathematical model is based on the following simplifications:

The input of batch equals the output of glass melt.

The batch floats on the glass melt as a continuous layer from the charging end to the position of melting ending.

The fresh glass on the batch layer penetrates into the batch and moves down to the tank.

The batch moves forward.

The temperature within each block is constant.

Heat transfer in horizontal directions can be neglected since the batch layer is relatively thin.

In the model, the primary thickness of the batch layer and the forward velocity changes with the change of method and the input of batch respectively. The process of batch melting is divided into the following steps: Temperature raising, melting beginning, melting and melting ending.

The mathematical formulation for the thermal balance of each block at different stages as shown in Fig. 3 are expressed as follows:

Block in the temperature-raising zone (all absorbed energy is used for raising temperature)

$$(Q_{fik} + Q_{gik})\Delta x\Delta z = \rho_b C_b H_b u_b \Delta z(T_{bi-lk} - T_{bik}) \quad (19)$$

Block of the melting beginning (absorbed energy partly used for raising temperature and partly for melting)

$$(Q_{fik} + Q_{gik})\Delta x\Delta z = \rho_b C_b H_b u_b \Delta z(T_{bi-lk} - T_m) + \rho_b Q_m u_b \Delta z(H_b - H_{bik}) \quad (20)$$

Block in melting zone (all absorbed energy used for melting)

$$(Q_{fik} + Q_{gik})\Delta x\Delta z = \rho_b Q_m u_b \Delta z(H_{bi-lk} - H_{bik}) \quad (21)$$

Block of melting ending (absorbed energy partly used for melting and partly for raising temperature)

$$(Q_{fik} + Q_{gik})\Delta x\Delta z = \rho_b Q_m u_b \Delta z H_{bi-lk} + \rho_b C_p H_{bi-lk} u_b \Delta z(T_{bik} - T_m) \quad (22)$$

RESULTS AND DISCUSSION

The results of the simulation models are shown in Fgs. 4 to 16. Fig. 4 illustrates the variation of NOx formation with inlet air temperature. As shown from the Fig. and expected from the theory, an increase in the air temperature increases the amount of NOx formation in the firebox. The formation of NOx increases with increasing the excess air for the combustion as presented in Fig. 5. The effect of air preheating and excess air on the adiabatic flame temperature is shown in Figs. 6 and 7. As illustrated from the Figs. increasing air temperature and decreasing excess air both increases the adiabatic flame temperature of the furnace. Figs. 8 and 9 show the variation of gas and wall temperatures at different regions in the furnace. As illustrated in Fig. 9 the first three zones of the furnace (6 meters from the inlet) have lower temperature compared with other zones. This is due to the

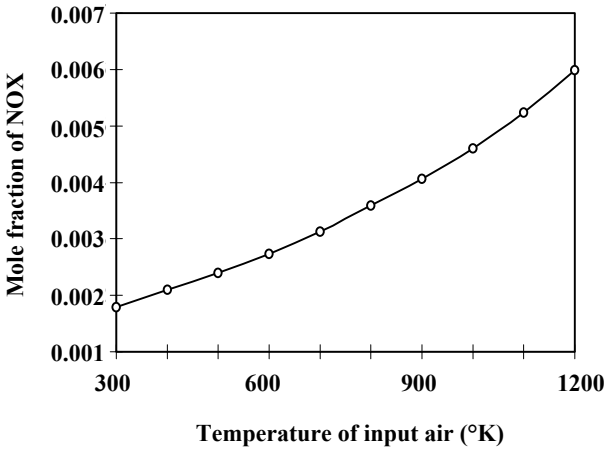

Fig. 4: Variations of mole fraction of NOx with temperature of inlet air

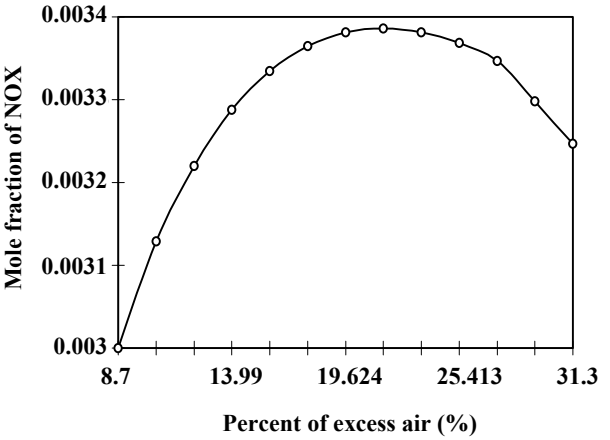

Fig. 5: Variations of mole fraction of NOx with percent of excess air

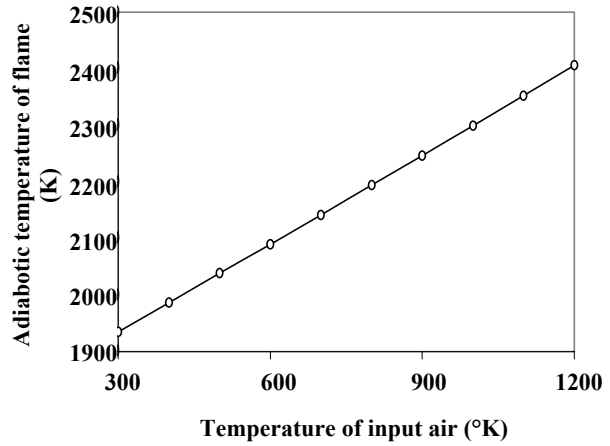

Fig. 6: Variations of adiabatic temperature of flame with temperature of inlet air

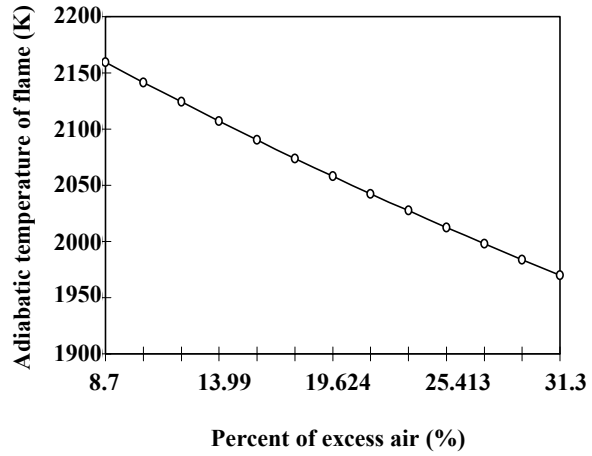

Fig. 7: Variations of adiabatic flame temperature with excess air

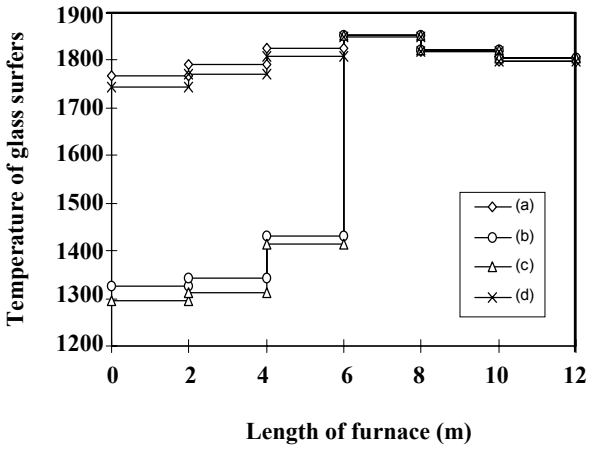

Fig. 10: Temperature distribution on the glass surface

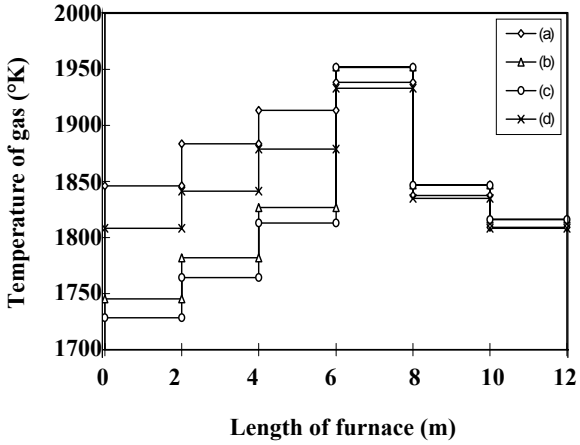

Fig. 8: Variations of gas temperature into the furnace with furnace length, a) first row near the burner, b) second row, c) third row, d) fourth row

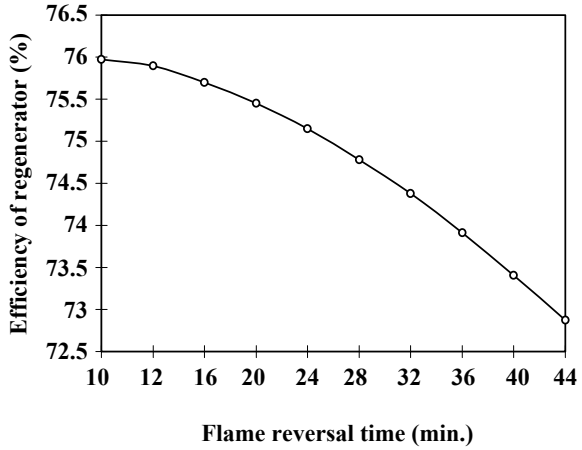

Fig. 11: Variations of regenerator efficiency with flame reversal time

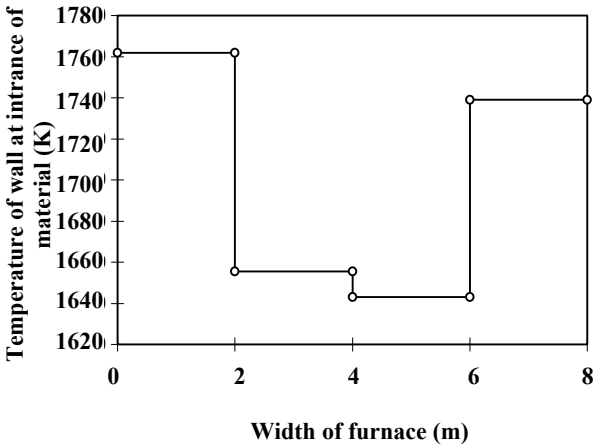

Fig. 9: Variations of wall temperature with furnace width

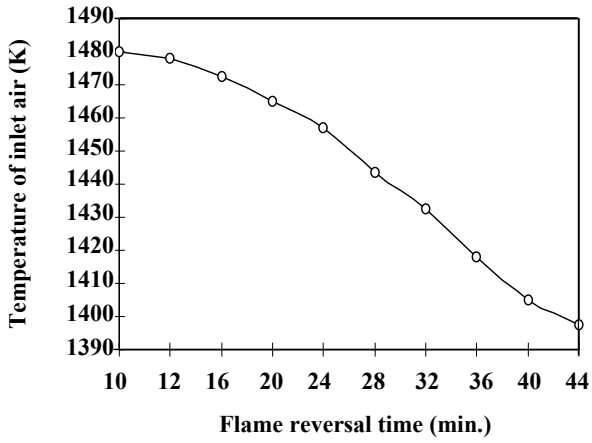

Fig. 12: Variations of temperature of inlet preheated air with flame reversal time

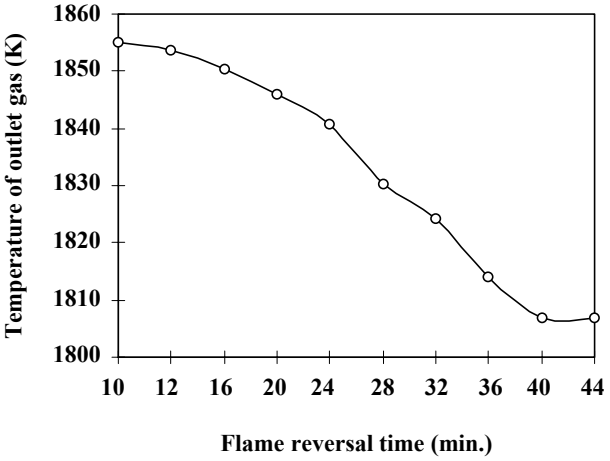

Fig. 13: Variations of temperature of outlet gas with flame reversal time

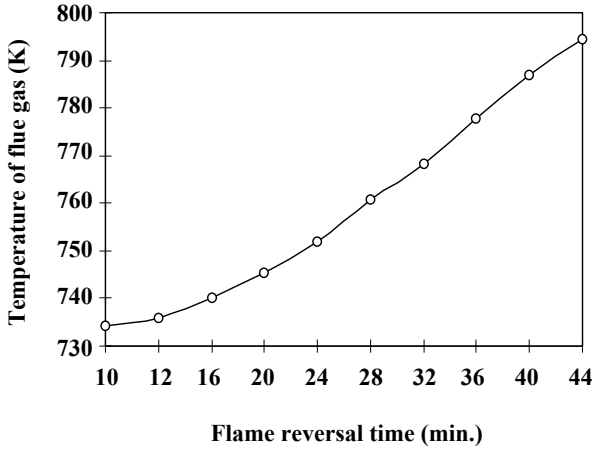

Fig. 14: Variations of temperature of flue gas with flame reversal time

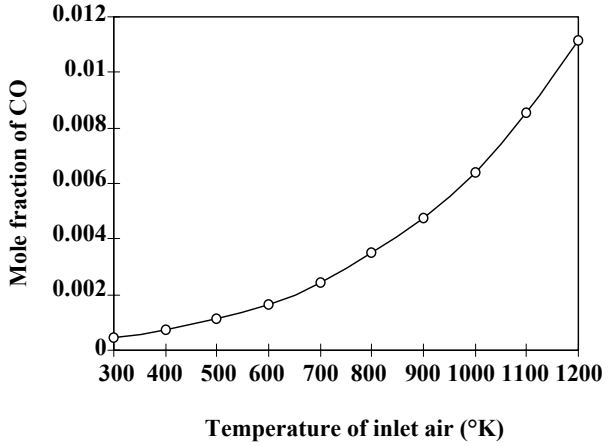

Fig. 15: Variations of mole fraction of CO with temperature of inlet air

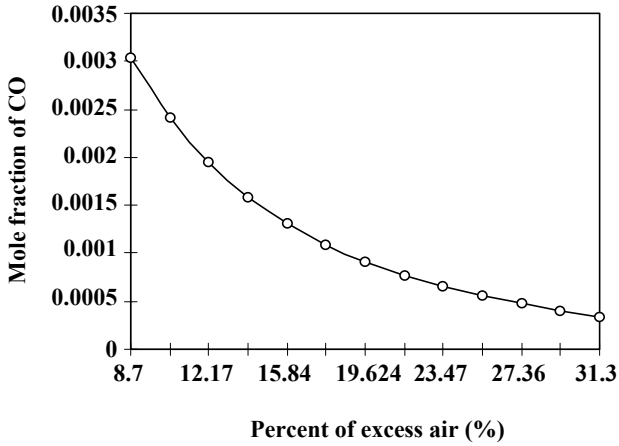

Fig. 16: Variations of mole fraction of CO with temperature of inlet air

inlet conditions in the furnace. Fig. 10 shows the variation of glass surface temperature along the furnace length at different zones. The results of regenerator's simulation are shown in Figs. 11 to 16. Variation of regenerator efficiency and air pre-heated temperature with the flame reversal time is presented in Fig. 11 and 12 which shows that efficiency and air temperature decreases with increasing the flame reversal time. This is due to decrease of the solid temperature and therefore increases the air and solid temperature difference, which results in lower efficiency. Figs. 13 and 14 show the variation of outlet and flue gas temperatures with flame reversal time. As can be observed from the Figs. the outlet gas temperature decreases with increasing flame reversal time which results lower efficiency. Figs. 15 and 16 illustrate the variation of CO with inlet air temperature and amount of excess air in the firebox. As expected, increasing air temperature and decreasing excess air both increase in CO formation in the furnace. The simulation programs now can be used for the optimization of furnace parameters and pollution control of the glass furnaces.

Nomenclature

A	Surface area, m^2
C_b	Specific heat of batch, J/kgK
C_p	Specific heat of glass melt, J/kgK
E	Emissive power, W/m^2

$\vec{G_iG_j}$	The directed flux areas between two gas zones, m^2
$\vec{G_iS_j}$	The directed flux areas between a gas and a surface zone, m^2
H_b	Primary height of batch layer, m
K	Gas absorption coefficient, m^{-1}
L	Regenerator bed length, m
$\dot{M}$	Mass flow rate, kg/s
Q_{fik}	Heat from combustion space, W/m^2
Q_{gik}	Heat from beneath melt, W/m^2
$\dot{Q}_{i\Leftrightarrow j}$	Radiative interchange between zones i and j, W
Q_m	Melting heat of batch, J/kg
$\dot{Q}_{(net)}$	Net radiative heat flow to a zone, W
S	Cross sectional area, m^{-1}
$\vec{S_iS_j}$	The directed flux areas between two surface Zones, m^2
T	Temperature, K
T_{bik}	Temperature of batch, K
T_m	Melting temperature of batch, K
u_b	Forward velocity of batch, m/s
v	Flow velocity, m/s
V	Volume, m^3
$\Delta x,\Delta z$	Mesh length in *x* and *y* directions, m

Greek letters

$\bar{\alpha}$	Lumped heat transfer coefficient, W/m^2K
ε	Emissivity
ρ	Density, kg/m^3
ρ_b	Packing density of batch, kg/m^3

Subscripts

b	Batch
bi-lk	Refer to blocks i to k
f	Fluid
g	Gas & glass
i	Incident
i , j , k	Iindicate the block positions in the x , y , z directions
m	Melting
s	Surface

Received : 6th September 2002 ; Accepted : 15th March 2004

REFERENCES

[1] McConnell, R. R. and Goodson, R. E., Modeling of a glass furnace design for improved energy efficiency, *Glass Tech.*, **20** (3) (1979).

[2] Hottel, H. C. and Sarofim, A. F., Rdiative transfer, Mc Graw Hill, (1967).

[3] Mase, H., Oda, K., Mathematical model of glass tank furnace with batch melting process, *J. Non-Crystalline Solids*, **38-39**, pp. 819 (1980).

[4] Carvalho, M. D. G. M. D. S., Lockwood, F. C., Mathematical simulation of an end-port regenerative glass furnace, *Proc. Inst. Mech. Engs.*, **199**, (1985).

[5] Sun, C., Song, L., A three dimensional mathematical model of a float glass tank furnace, *Glass Technology*, **36** (6) p. 213 (1995).

[6] Wang, J. et al., Validation of an improved batch model in a coupled combustion space/melt/batch melting glass furnace simulation, *Glasch Ber Glass Sci. Technologi*, **73** (10) p. 299 (2000).

[7] Rhine, J. M., Tucker, R. J., "Modeling of gas fired furnace and boilers", Mc Graw Hill, (1991).

[8] Sadrameli, S. M., PhD thesis, University of Leeds, Leeds, U.K. (1988).

[9] Hausen, H., "Heat transfer in counter flow, parallel flow, and cross flow", McGraw Hill Co., New York, (1983).